The final publication is available at

https://dx.doi.org/10.1039/c4tb01108b

Additional Information

Site-specific immobilization of DNA on silicon surfaces by thiol-yne reaction

Jorge Escorihuela, María-José Bañuls, Rosa Puchades and Ángel Maquieira*

Covalent immobilization of ssDNA fragments onto silicon-based materials was performed using the thiol-yne reaction. Chemical functionalization provided alkyne groups on the surface where the thiol-modified oligonucleotide probes can be easily photoattached as microarrays, reaching an immobilization density around 30 pmol·cm^{-2}. The developed method presents the advantages of spatially controlled probe anchoring (by using a photomask), direct attachment without using cross-linkers, and short irradiation times (20 min). Hybridization efficiencies up to 70%, with full complementary strands, were reached. The approach was evaluated by scoring single nucleotide polymorphisms with a discrimination ratio around 15. Moreover, the potential applicability of the proposed methodology is demonstrated through the specific detection of 20 nM of a genomic target of bacterial *Escherichia coli*.

1. Introduction

Over the past decades, advances in the technologies and methods for rapid detection of sequence specific genes have been achieved[1,2] and applied in clinical diagnosis or environmental monitoring, among others.[3] Thus, the microarraying of nucleic acids on solid supports has become an area of fundamental interest.[4] Particularly, microarrays are an alternative to homogeneous assays because they allow easy continuous monitoring and miniaturization. In the last years, nucleic acids have been immobilized on surfaces, both noncovalently and covalently.[5] In this regard, noncovalent immobilization has been achieved by means of physical adsorption[6] and biospecific interactions (e.g. avidin-biotin).[7] Covalent immobilization, however, results in more robust arrays, and is of great interest for many bioanalytical and medical applications.[8]

Regarding the material nature, silicon based supports, including glass, are very appropriate for DNA microarraying because of their high stability at different temperatures, inertness to many chemicals and solvents, good optical properties, low fluorescence absorbance that yields high signal-to-noise ratio, versatile chemical functionalization, low surface roughness, better spot uniformity, and compatibility with CMOS technology, which facilitates the fabrication of lab-on-a-chip devices.

In all biosensing applications involving silicon, one of the critical steps is the probe anchoring to the support. This needs the chemical surface functionalization, which provides active functional groups on the surface, and is almost exclusively done with organosilanes. The most common surface functionalities are carboxy, epoxy, thiol and amine, but the procedures for tethering the DNA require long times and the use of crosslinkers. So, developing immobilization strategies being robust, rapid and efficient, especially those allowing site-specific anchoring of probes at defined locations is still demanded.[9]

Because of its *"click"* chemistry properties, including high yields, regiospecificity, mild reaction conditions, and tolerance to a variety of functional groups,[10,11] thiol-ene reactions have been used recently as an elegant procedure for biomolecules immobilization with very good performance.[12] Less exploited but equally interesting is the thiol-yne reaction, which presents the same "click reaction" advantages as thiol-ene, and it is faster than the corresponding TEC reaction.[13] Also, it allows the addition of two thiol moieties giving a double addition product, which mean higher surfaces functionalization densities and increases the stability. However, few examples of this reaction for biomolecule immobilization on solid supports have been reported.[14]

In this paper we study for the first time the use of thiol-yne reaction to efficiently perform rapid, fast and efficient DNA microarrays on silicon. Since the thiol-yne reaction allows covalent attachment of two thiolated molecules to an alkyne, it appears to be perfectly suited to obtain high surface densities of probe on the interface. The thiol- ended oligonucleotides can be directly attached to the support, and the patterned surfaces can effectively discriminate SNPs and bacterial DNA.

2. Materials and methods

2.1. Materials.

The silicon-based wafers were provided by the Valencia Nanophotonics Technology Center (NTC) at the Universitat Politècnica de València (Spain) as 2 μm thick silicon oxide layer grown on (1 0 0) silicon wafer. Hydrogen peroxide (35% w/w), 3-glycidoxypropyl trimethoxysilane (GOPTS) and propargylamine were purchased from Sigma-Aldrich Química (Madrid, Spain). Toluene, 2-propanol and sulfuric acid 95-98% were purchased from Scharlau (Madrid, Spain). Note: All the chemicals should be handled following the corresponding material safety data sheets. Oligonucleotide sequences (Table 1) were acquired from Eurofins Genomics (Ebersberg, Germany). DNA concentration and quality were determined by measuring the optical density at 260/280 nm with a NanoDrop ND 1000 Spectrophotometer (Thermo Fisher Scientific, Wilmington, Delaware). Milli-Q water with a resistivity above 18 mΩ was used to prepare aqueous solutions. The buffers employed, phosphate buffer saline (1×PBS, 0.008 M sodium

phosphate dibasic, 0.002 M sodium phosphate monobasic, 0.137 M sodium chloride, 0.003 M potassium chloride, pH 7.5), PBS-T (10×PBS containing 0.05% Tween 20), saline sodium citrate (10×SSC, 0.9 M sodium chloride, 0.09 M sodium citrate, pH 7) and carbonate buffer (10×CB, 0.5 M sodium carbonate, pH 9.6) and washing solutions were filtered through a 0.22 μm pore size nitrocellulose membrane from Whatman GmbH (Dassel, Germany) before use.

2.2 Instrumentation

Microarray printing was carried out with a low volume non-contact dispensing system from Biodot (Irvine, CA, USA), model AD1500. Contact angle system OCA20 equipped with SCA20 software was from Dataphysics Instruments GmbH (Filderstadt, Germany). The measurements were done in quintuplicate at room temperature with a volume drop of 5 μL employing 18 mΩ water quality. X-ray photoelectron spectra were recorded with a Sage 150 spectrophotometer from SPECS Surface Nano Analysis GmbH (Berlin, Germany). Non-monochromatic Al Kα radiation (1486.6 eV) was used as the X-ray source operating at 30 eV constant pass energy for elemental specific energy binding analysis. Vacuum in the spectrometer chamber was 9×10^{-9} hPa and the sample area analyzed was 1 mm^2. Atomic force microscopy (AFM) images were obtained with a Veeco model Dimension 3100 Nanoman (Veeco Metrology, Santa Barbara, CA, USA) using tapping mode at 300 kHh. Imagining was performed in AC mode in air using OMCL-AC240 silicon cantilevers (Olympus Corporation, Japan). The images were captured using tips from Nano World with a radius of 8 nm. The AFM images were obtained at room temperature in air under ambient conditions. IRRAS spectra were recorded on a Bruker Tensor 27 FT-IR spectrometer using a commercial variable angle reflection unit (Auto Seagull, Harrick Scientific). All spectra were obtained at an incident angle of 68° with 2048 scans recorded for each sample. The fluorescence signal of the spots was registered with a homemade surface fluorescence reader (SFR) having a high sensitive charge couple device camera Retiga EXi from Qimaging Inc, (Burnaby, Canada), with light emitting diodes Toshiba TLOH157P as light source.[15] For microarray image analysis and subsequent quantification, GenePix Pro 4.0 software from Molecular Devices, Inc. (Sunnyvale, CA, USA) was employed.

2.3. Methods

2.3.1. Silanization of slides

Si-based wafers were cut into pieces of 2×1 cm and systematically cleaned with piranha solution (H$_2$SO$_4$:30% H$_2$O$_2$ 3:1 v/v) for 1 h at 60 °C to remove organic contaminants. Caution: Piranha solutions react violently with organic materials and should be handled with extreme care. This treatment was followed by three rinsings with deionized water and drying under a filtered air stream. To introduce reactive functional groups, chip were immersed under an argon atmosphere into a solution of GOPTS 2% in toluene for 2 h at room temperature. After, samples were withdrawn from the silane solutions and washed several times with 2-propanol and then dried under nitrogen stream. Next, the chips were baked for 10 min at 150 °C and stored under inert atmosphere. For alkyne derivatization, chips were immersed under argon atmosphere into a solution of 10 μL of propargylamine with 1 mL of dry toluene and left 4 h at room temperature. Finally,

samples were washed several times with CH$_2$Cl$_2$ and then dried under air stream.

2.3.2. Oligonucleotide immobilization

Silicon-oxide slides were treated following the above described procedure to obtain the corresponding alkyne-functionalized slides. To perform this study, oligonucleotide probes A and B (Table 1), consisting in 5' SH-, 3' Cy5 oligomers, were used to evaluate the platform efficiency towards oligonucleotide immobilization. For that, different probe A and B concentrations in 1×PBS were prepared (40 nL) onto the alkyne-functionalized surface and exposed to UV-light at 365 nm, with a mercury capillary lamp (6 mW·cm^{-2}, Jelight Irvine, CA, USA) placed at a fixed distance (<0.5 cm) from the slide, for 20 min to induce the immobilization. Finally, slides were thoroughly rinsed with PBS and water, and air dried. Immobilization results were obtained from the fluorescence signals using SFR.

Table 1. Nucleotide sequence of probes and target.

Name	sequence (5' to 3')	5' end	3'end
Probe A	(T)$_{15}$-CCCGATTGACCAGCTAGCATT	SH	Cy5
Probe B	CCCGATTGACCTGCTAGCATT	SH	Cy5
Probe C	(T)$_{15}$-CCCGATTGACCAGCTAGCATT	SH	none
Probe D	(T)$_{15}$-CCCGATTGACCTGCTAGCATT	SH	none
Probe E	(T)$_{15}$-CCCGATTGATTAGCTAGCATT	SH	none
Probe F	(T)$_{15}$-CCATATTGACCAGCTATCATT	SH	none
Probe G	(T)$_{15}$-CGCCGATAACTCTGTCTCTGTA	SH	none
Probe H	(T)$_{15}$-TTCACGCCGATAACTCTGTCTCT	SH	none
Target A	AATGCTAGCTGGTCAATCGGG	Cy5	none
Target B	AATGCTAGCTAATCAATCGGG	Cy5	

2.3.3. Hybridization assays

For the hybridization assays, silicon-based slides were alkyne-functionalized as described above. Serial dilutions of Probe C (from 0.01 to 2 μM) in 1×PBS were spotted (40 nL) onto the functionalized slides creating the microarray (four spots/concentration). Then slides were exposed to UV-light at 365 nm for 20 min, washed with water and air-dried. After washing, 50 μL of Target A (concentrations ranging from 100 pM to 1 μM in 1×SSC) were spread out with a coverslip. After incubation in a slim box for 1 h at 37 °C, the coverslip was gently removed and the chip washed with PBS-T and deionized water. The fluorescence intensity of the spots was registered using SFR.

2.3.4. Reusability of the functionalized chips

To study the reusability on the developed platform, silicon-based slides were alkyne-functionalized as described above. Afterwards, Probe C, at different concentrations in 1×PBS was microarrayed (4×5 spots, 40 nL/spot) onto the functionalized slides creating the microarrays. Then slides were exposed to UV-light at 365 nm (6 mW/cm^2) for 20 min. The slides were washed with PBS and water, and air-dried. After washing, 50 μL of the complementary oligonucleotide 5' Cy5-labeled (Target A) dissolved in 1×SSC were spread under a coverslip and incubated in a dark and humidified chamber for 1 h at 37 °C. After rinsing and drying, the fluorescence intensity of the spots was displayed by means of SFR. Then, the chip was washed with MES buffer (pH 6.5) and ethanol to remove

hybridized target oligonucleotide from the surface. After checking by SFR that complementary strand was fully dehybridized, a new hybridization cycle was started. For that, Target A (in 1×SSC) was spread out with a coverslip and incubated under the described hybridization conditions, then washed and read by SFR.

2.3.5. Detection of mismatches

Four oligonucleotide sequences, Probes C, D, E, and F having zero, one, two and three base mismatches for Target A, respectively, were microarrayed (4×4 spots, 40 nL/spot) onto the alkyne-functionalized silicon oxide chip. After probe immobilization as described above, the microarray was subjected to hybridization with Target A (from 0.5 to 200 nM) in SSC under different stringency conditions for 1 h at 37 ºC. After washing and drying, the fluorescence was measured with SFR.

2.3.6. Detection of bacterial *Escherichia coli*

Silicon-based slides were alkyne functionalized as described above. Then, solutions containing SH-labeled Probe G (E. coli specific probe) and Probe H (control probe) were spotted onto the functionalized slides creating the microarray. Afterwards, slides were exposed to UV-light at 365 nm for 20 min and subsequently washed and air-dried. Cy5-labeled PCR duplexes were firstly melted by 10 min incubation at 95 °C, followed by fast cooling for 1 min on ice. Then, PCR product solutions (50 µL) in hybridization buffer (1×SSC) were distributed on the chip. After incubating 1 h at 37 °C, the slides were washed with PBS-T, rinsed with deionized water, and air dried.

2.3.7. General Procedure for DPI measurements

Before the DPI experiments, the unmodified silicon oxynitride AnaChip (Biolin Scientific, Stockholm, Sweden) was alkynyl-functionalized under the above described conditions, and Probe C (1 µM) was photoimmobilized. Then, the chip was inserted in the device and calibrated as described elsewhere.[16] After that, the hybridization experiment was started. The running buffer was 1×PBS at a flow rate of 50 µL/min, and the temperature was set at 20 °C. First a non complementary strand was flowed over the chip (50 µL, 1 µM, 10 µL/min) followed by running buffer for 5 min. Then, 250 µL of 1 µM complementary DNA, Target A, in 1×PBS were injected at 10 µL/min. After flowing running buffer for several minutes, two additional injections of Target A were performed (50 µL, 1 µM, 10 µL/min). Analysis of refractive index, thickness and mass per unit area on the sensor chip surface was achieved using the AnaLight Bio200 software (Biolin Scientific, Stockholm, Sweden).

3. Results and discussion

DNA immobilization assays

A thiolated probe was investigated for its reactivity with alkynyl-terminated silicon surfaces under photochemical irradiation. Fig. 1 depicts schematically the different surface modification steps performed using the proposed methodology. First, silicon slides were cleaned with piranha solution and

functionalized with 3-glycidoxypropyltrimethoxy silane for 2 h. Next, the epoxy-terminated chip was immersed into a propargylamine solution for several hours, to give the desired alkynyl-terminated surface. The reaction was followed by means of water contact angle (WCA) measurements and no significant variations were observed for reaction times longer than 4 h. Initially, a rapid increase of the WCA was observed during the first 10 min, followed by a slight variation for the first 2 h, reaching a plateau at 3.5 h. The final conditions were set at 4 h (Fig. S1, ESI†).
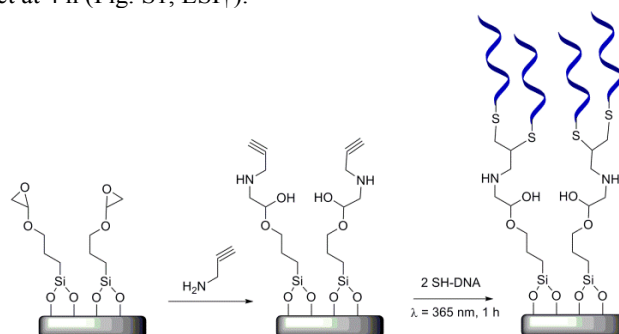
Fig. 1 Reaction scheme for the immobilization of thiolated DNA on the propargylamine-modified surface by photoinitiated thiol-yne reaction.

To demonstrate the use of thiol-yne chemistry to mediate DNA immobilization, a 3' Cy5-labeled, 5' thiol-ended probe (Table 1, Probe A) was microarrayed (4×8 spots, 40 nL/spot) at different concentrations (from 0.01 to 2 µM) onto the alkyl-terminated substrate. Initially, irradiation time was investigated and the best results in terms of fluorescence intensity were obtained for UV exposure times longer than 10 min (Fig. S2, ESI†). After irradiation (365 nm, 20 min) of the non thiol-modified oligonucleotide (Target A), used as a nonspecific adsorption control, no measurable immobilization signal was detected. Furthermore, no significant fluorescence was observed when amine-functionalized Cy5-labeled probes were spotted and incubated over the functionalized surface, confirming the propargylamine efficient coating on the epoxy-terminated surface. Finally, it was also observed that less than 2% of the thiolated oligonucleotide was anchored to the solid support when performing the immobilization experiment without irradiation after 1 h incubation in the dark.

Next, immobilization efficiency of Probes A and B (from 0.01 to 2 µM) was established from the corresponding standard calibration curve as described elsewhere (Fig. S3, ESI†).[12h] It is worth mentioning that although both probes have the same base sequence, Probe A contains a poly T spacer. Under the studied conditions, maximal immobilization densities of 29.7 and 27.8 pmol·cm^{-2} were reached for Probes A and B at 2 µM, respectively (Fig. 2). These densities were higher than those reported by other authors working on different materials.[17] The difference between Probe A and B was not large enough to point to a key role of the poly T chain in the probe anchoring performance. However, we decided to use as far as possible oligonucleotide probes containing the poly T arm as this could facilitate the hybridization event.
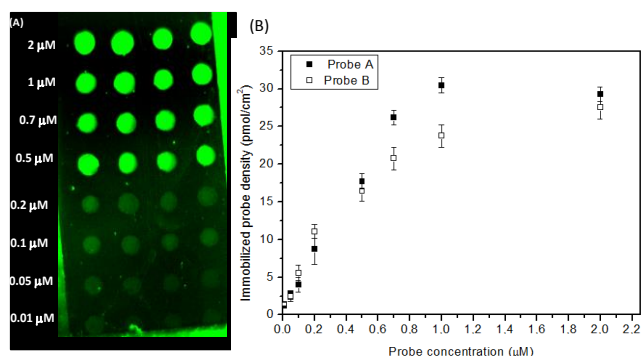
Fig. 2 (A) Array image for immobilization of probe A. (B) Oligonucleotide immobilization densities for probes A and B vs spotted probe concentration.

The higher hydrophobicity of the alkynyl-terminated surface, in comparison with the alkenyl-[12h] and epoxy-ended[18] surfaces, led to smaller spot sizes, as shown in Table 2 (Fig. S4 and S5, ESI†). These results support the potential application of thiol-yne chemistry for the construction of highly dense DNA microarrays.

Table 2. Water contact angle values (WCA) and DNA microarray spot average diameter for surfaces functionalized with epoxy, alkene and alkyne groups.

Name	Epoxy	Alkene	Alkyne
WCA (º)	56 ± 2	84 ± 2[a]	103 ± 3
Diameter (μm)	353 ± 25	288 ± 23	195 ± 23

[a] Data from reference 12h.

Spatially controlled binding of biomolecules on solid surfaces is of paramount importance in the development of biosensors.[19] In the last years, photolithographic methods have been efficiently used to selectively construct DNA arrays by UV exposure on different substrates.[20] The use of photolithography to constructively pattern a DNA-functionalized on the alkyne-terminated surface was demonstrated by means of irradiation through a photomask. For this purpose, Probe A at 1 μM in 1×PBS was spread out onto the alkynyl-functionalized slide, which was covered immediately with the photomask and irradiated at 365 nm for 20 min. After washing, the fluorescence was read by SFR showing the patterned features (Fig. 3). The proposed photochemical approach afforded spatial control on the probe attachment reaction, allowing a site-specific immobilization of thiolated oligonucleotides by radical reaction of thiolated oligonucleotides and alkyne surfaces.
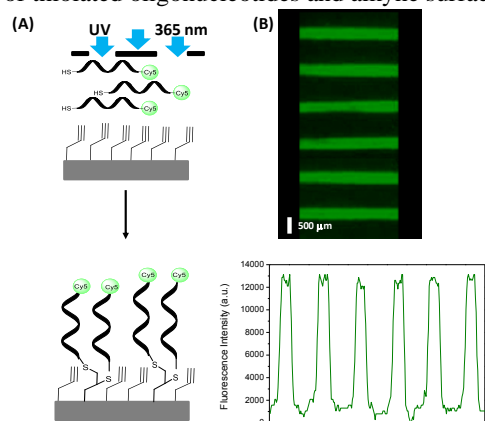
Fig. 3 (A) Schematic illustration of the surface patterning with a photomask. (B) Fluorescence image of the patterned surface and contrast profile.

Surface characterization

The different functionalized surfaces were characterized by several techniques (contact angle measurement, infrared reflection-absorption spectroscopy (IRRAS), X-ray photoelectron spectroscopy (XPS), and tapping mode atomic force microscopy (TM-AFM).

The initial bare silicon slide had a contact angle below 10º after treatment with the piranha solution, which was attributed to the high-density of hydroxyl groups generated on the surface by the oxidation treatment (Fig. S4, ESI†). Upon functionalization with GOPTS, the WCA significantly increased to 56º; and when reacting with propargylamine, the alkyl-terminated surface showed a contact angle of 103º, confirming the high hydrophobicity of the modified surface. Finally, after covalent attachment of DNA by means of the thiol-yne reaction, the contact angle dropped to 50º, in accordance with the values reported by different authors.[21]

XPS was used to evaluate the chemical composition of the silicon surface after each treatment and the nature of the chemical bonding associated with transformations that occurred on the surface. Surface chemical composition calculated from high-resolution XPS spectra is shown in Table S1. Organosilane attachment to the surface resulted in a decrease in the Si signal and an increase in the C 1s signal compared to the raw material (Fig. S6, ESI†). After DNA immobilization, Si, N, C, and O content changed only slightly, compared to epoxy and alkyl-terminated Si surfaces. Measurable sulphur was only detected on the DNA-immobilized slide.

The narrow scan of C1s signal was used to probe the chemical states of carbon on the surface (Fig. 4 and Fig. S7 ESI†). For epoxy-functionalized surfaces, the C1s signal can be deconvoluted into three components, where the two main were centred at 286.5 and 284.7 eV, and were assigned to C-O, and C-C carbon atoms, respectively. All electron binding energies of the different type of carbon peak positions were derived from the literature for other similar systems.[22] The deconvolution of C1s peak for the alkynylated surface after propargylamine treatment showed an increase in the ratio between the two main bands (284.7 and 286.5 eV) due to the elongation of the hydrocarbon chain in comparison with the epoxylated surface. More importantly, a new peak contribution was detected at 285.9 eV, attributable to C-N bonds. For the DNA-functionalized surface, the C 1s peak showed three main features, firstly an increase of the C-C contribution; secondly, an increase of C-N and C-S contribution (285.9 eV) in comparison with C-O contribution (286.5 eV); and thirdly, an additional new band at 289.0 eV corresponding to C=O carbon atom (Fig. 4), which represent carbon species specific to the DNA bases.[23] All this features indicated the success in the oligonucleotide attachment. Complementarily, IRRAS analysis of the alkyne-terminated surface showed the symmetric and antisymmetric methylene C-H stretching frequencies at 2854 and 2925 cm^{-1}, respectively. Additionally, a peak at 3326 cm^{-1} characteristic of the C≡C-H stretching was observed, indicating the presence of terminal alkyne moieties on the surface (Fig. S8, ESI†)

The roughness and morphology of the modified surfaces were evaluated using TM-AFM (Table S2 and Fig. S9, ESI†). The rms roughness of the piranha cleaned slide was 0.28 nm, which is in the range reported in literature for cleaned

surfaces.[24] The rms roughness after GOPTS condensation (0.21 nm) did not change significantly with respect to the cleaned surface, indicating the formation of a silane monolayer rather than a multilayer. After propargylamine and ssDNA attachment, the rms values increased to 2.10 and 3.24, respectively.
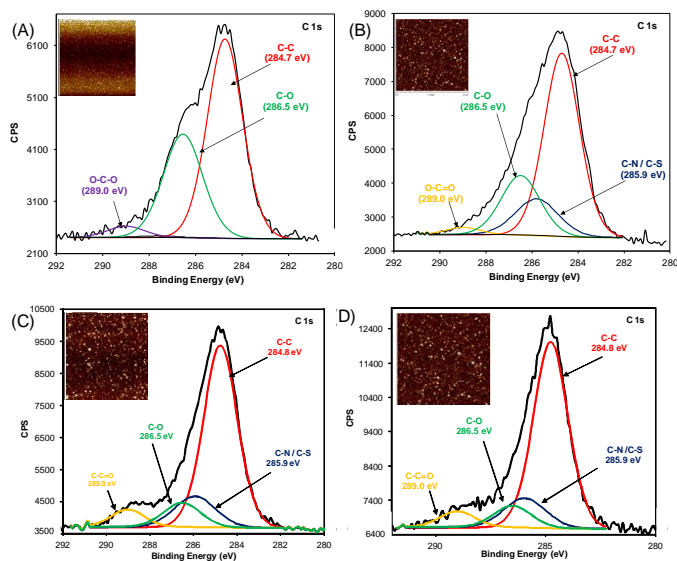
Fig. 4 XPS high-resolution C 1s spectrum and AFM images (inlet) of (A) epoxy, (B) alkyne, and (C) DNA single strand and (D) double strand modified silicon surfaces.

DNA hybridization assays

The bioavailability of the probes attached following the proposed methodology was assessed through hybridization assays, and the sensitivity and selectivity were established. Thiol-ended Probe C was immobilized and the hybridization was carried out with Cy5-labeled fully complementary strand (Target A) in 1×SSC. First, the influence of parameters such as time and temperature on hybridization was studied (Fig. S10 and S11 ESI†); best results in terms of fluorescence intensity were obtained when performing the hybridization assays at 37 ºC during 1 hour. Next, hybridization sensitivity was evaluated at different Probe C (0.01 to 2 μM) and Target A (1 nM to 1 μM) concentrations. Hybridization signal intensities increased at higher probe concentrations (0.01 to 1 μM). A non-complementary Cy5-labeled DNA strand showed negligible nonspecific hybridization.

The maximum amount of hybridized DNA, 21.7 pmol/cm^2, was obtained from the calibration curve (Fig. S12, ESI†), and corresponds to 1.3×10^{13} molecules of DNA/cm^2. This density is similar to the previously reported on other substrates for DNA microchip technology,[25] and means a hybridization yield of 70%. These data were obtained with a spotting probe concentration of 2 μM and a target concentration of 1 μM. Hybridization signal increased with target concentration, reaching saturation at 2 μM probe concentration in all the cases. Depending on the immobilized probe density, hybridization efficiencies varied from 20 to 71% (Fig. S13, ESI†).

For probe spotting concentrations higher than 1 μM, the detection limit of target concentration was 90 pM, estimated as the concentration that gives a fluorescence signal three times the standard deviation of the signal obtained with a noncomplementary strand. This excellent detection limit was attributed to the small spot size and to the high immobilization density obtained with the proposed approach.

The bioavailability of the immobilized probes on the alkyne-terminated silicon surface was evaluated within a period of eight weeks. For these experiments, a batch of chips was prepared and two of them were analyzed every week, storing the rest inside a slim box at 4 °C during this period. Taking as reference the signal intensity obtained in the assay developed on the first week, the signal intensity profile indicated that the array was active for eight weeks as minimum without significant loss of activity (Fig. S14, ESI†). Finally, the ability to use and reuse the same functionalized substrate via dehybridization was assayed.[26] Interestingly, chips could be used for five consecutive runs with only a minor loss in the fluorescence intensity (only 7% from the first experiment). These results confirm the robust covalent bond between the oligonucleotide and the functionalized surface through the thiol-yne reaction and the more stable packed surface modification obtained by means of the thiol-yne reaction.

Dual polarization interferometry

In order to gain more information about the hybridization process, both strategies were analyzed by dual-polarization interferometry (DPI).[27] This technique is an effective analytical approach for real-time, label-free measurement, allowing unambiguously quantitative monitoring of changes in mass, refractive index (RI) and thickness on a sensor surface due to the binding of the analyte to the immobilized biomolecule.[28]

For that purpose, unmodified Analight chips were functionalized with alkynyl groups following the surface modification protocol optimized in the microarray format, and Probe C (1 μM), was photoimmobilized on the sensing surface as described above. After that, hybridization with the complementary strand was monitored by flowing Target A, at 1 μM in 1×SSC, for 25 min in a first round, and for 5 min in the second and third injections. Changes in RI, mass density and layer thickness during the process were analyzed. The hybridization yield was estimated as 21% and 24.5% after the first and second injection, respectively. No significant hybridization was detected after the third injection. In order to calculate the hybridization yield, the probe density obtained in microarray, for the same immobilization conditions (28.4 pmol/cm^2), was used. Next, for the demonstration of the specificity of the hybridization, a non complementary strand was flowed over the chip previously to the complementary strand and no surface changes were observed (Fig. S15, ESI†).

Considering as reference the ideal situation of a close packed monolayer of the dsDNA linked orthogonal to the surface (43.7 pmol/cm^2 and a layer thickness of 8.9 nm), the mass density after the first injection fits with a 13% of such close packed monolayer (CPM). This should provide a layer average thickness of 1.16 nm; the measured thickness, 0.73 nm, indicates that the dsDNA is not standing orthogonal to the surface but with a tilt angle of 39º. This is corroborated with the obtained thickness data after the second and third injections, respectively. The DPI data (Table 3) correlate well with those obtained in microarray format, and with previously reported data.[12h,29]

Table 3. Numbers extracted from DPI experiment

	Complementary Strand Injection Round		
	1	2	3
Density (g/cm^3)[a]	0.556	0.549	0.543
Thickness (nm)[a]	0.729	0.868	0.899

Mass (ng/mm²)[a]	0.405	0.477	0.489
Surf. Dens. (pmol/cm²)[b]	5.91	6.95	7.12
Hybridization yield (%)[c]	21	24	25
% CPM[d]	13	16	16
Tilt angle (o)[e]	39.0	38.7	38.6

[a] Values provided directly by the Analight. [b] Complementary strand surface coverage, calculated from the mass (ng/mm²) and the molecular weight. [c] Hybridization yield calculated from the surface density and the immobilized probe determined by microarray (28.4 pmol/cm²). [d] Surface coverage degree regarding a dsDNA close packed monolayer standing orthogonal to the surface (43.7 pmol/cm²). [e] Tilt angle extracted from the experimental and expected thickness for the % CPM obtained standing orthogonal to the surface.

Demonstration of single-base mismatch differentiation capability

Single nucleotide polymorphisms (SNPs) are the most abundant form of genetic variation in the human genome, with estimates of more than 10 million common SNPs.[30] The single nucleotide changes in human genes may cause genetic disorders. Therefore, the accurate and robust detection of such SNPs plays a central role in the field of DNA diagnostics.[31]

The selectivity of the present approach was evaluated through hybridization with different oligonucleotide probes containing mismatched sequences towards Target A (Probes C, D, E and F, Table 1). In this assay, a full complementary (PM) and three mismatched (MM1, MM2 and MM3) oligonucleotide probes, were immobilized onto an alkinyl-functionalized slide. After washing, the hybridization with Target A at 50 nM concentration was done. Working under stringency conditions, by adding formamide from 0% to 30% (v/v), discrimination was possible reaching a maximum discrimination ratio of 14.3 (Fig. 5A). This result is in the range of those achieved with other approaches for oligonucleotides of similar length.[32] Negligible responses (S/N < 3) were obtained when assaying 5 and 10 base-pair mismatch targets for a broad range of concentrations (from 0.5 to 200 nM). An increase of the ionic strength of the hybridization buffer (3×SSC) resulted in a worsening of the discrimination efficiency (Fig. S16, ESI†), whereas a decrease of the ionic strength (0.1×SSC) allowed us to discriminate one single nucleotide mismatch lowering the formamide content. The results indicate that under the described conditions, the sensor exhibits enough capability for distinguishing a single-base mutant sequence.

Detection of bacterial *E. coli*

To proof that the proposed methodology was good for developing biochips to detect bacterial infection, Probe G was immobilized. The nucleotide sequence of Probe G was complementary to the central region of 300 bp amplicon specific to detect an innocuous serotype of *E. coli*, a versatile bacterium with a number of unique features.[33] Although most *E. coli* strains are harmless, some serotypes are pathogenic and can cause serious food poisoning in humans.

Thus, the mentioned *E. coli* probe (Probe G, 1 μM) and another non-specific sequence (Probe H, 1 μM) used as control, were immobilized onto a functionalized slide creating the microarray (Fig. S17, ESI†). Then, the Cy5-labeled PCR product (about 300 bp) from the lysis of E. coli bacteria (20 nM in 1×SSC) was hybridized for 45 min at 37 °C. As can be seen, the resulting assay was highly specific for the bacteria; the spots corresponding to the specific probe showed fluorescence, whereas no fluorescence signal was observed in negative controls, which indicates no false positive results.

For the evaluation of intrachip and chip-to-chip relative standard deviations, the signals obtained after the analysis of PCR products corresponding to 100 nM were analyzed. The intrachip RSD varied from 5 to 8%, whereas for the chip-to-chip RSD ranged from 8 to 10%. These results corroborate the good performances of the arrays to detect genomic DNA at very low levels.

One extra assay was performed in chips containing a mix of probes. For that, alkenyl-chips were prepared following the described methodology and three different probes (probe E, A and G) were immobilized by thiol-yne chemistry. Next, hybridization was performed using complementary oligonucleotide sequences to Probe A in one case (Target B), and Probe G (*E. Coli* PCR products) in another. As can be seen in Fig. 5B, selective hybridization was successfully achieved, with very low backgrounds and no cross-contamination. As expected, when a mix of both targets was hybridized, all the spots in the microarray provided fluorescence.
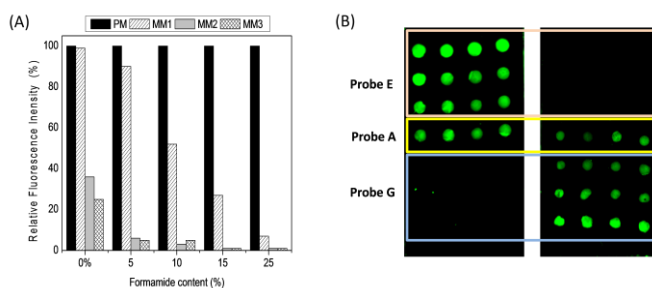
Fig. 5 (A) Effect of formamide in the detection of SNPs. (B) Fluorescence image of a "mix of probes chip" hybridized with Target B (left hand) and with *E.coli* PCR products (right hand).

4. Conclusions

The thiol-yne reaction was successfully applied for surface modifications to generate oligonucleotide microarrays with a site-specific location on the functionalized silicon surface. This direct covalent attachment of oligonucleotides chemistry on silicon-based surfaces is fast, clean and compatible with aqueous media chemistry, which is a crucial parameter for its bioutility. Based on this methodology, the constructed arrays exhibited high sensitivity, good selectivity, and reliability. As a proof-of-concept, the detection of PCR amplified DNA products was also demonstrated. Moreover, the limits of detection are very low and comparable to those reported in the literature using fluorescent, enzymatic or metal nanoparticle labels on different supports. The robustness, stability and the fact that it can be patterned and locally addressed makes the proposed strategy very promising as a universal platform for the development of silicon-based integrated optical biosensors, which could possibly be used widely in potential applications.

Notes and references

Centro de Reconocimiento Molecular y Desarrollo Tecnológico, Departamento de Química, Universitat Politècnica de València, Camino de Vera s/n, 46022 Valencia, Spain. Fax: +34 963879349; Tel: +34 963879349; E-mail: amaquieira@qim.upv.es

1   (a) F. S. Collins, E. D. Green, A. E. Guttmacher and M. S. Guyer, *Nature*, 2003, **422**, 835–847; (b) I. Huys, G. Matthijs and G. Van Overwalle, *Nat. Rev. Genet*. 2012, **13**, 441–447.

2   J. I. Cutler, E. Auyeung and C. A. Mirkin, *J. Am. Chem. Soc*. 2012, **134**, 1376–1391.

3   J. W. Liu, Z. H. Cao and Y. Lu, *Chem. Rev*. 2009, **109**, 1948–1998.

4   (a) B. R. Jordan, *Expert Rev. Mol. Diagn*. 2010, **10**, 875–882; (b) X. Li, R. J. Quigg, J. Zhou, W. Gu, R. P. Nagesh and E. F. Reed, *Curr. Genomics* 2008, **9**, 466–474; (c) A. Sassolas, B. D. Leca-Bouvier and L. J. Blum, *Chem. Rev*. 2008, **108**, 109–139.

5   V. Singh, M. Zharnikov, A. Gulinoc and T. Gupta, *J. Mater. Chem*. 2011, **21**, 10602–10618.

6   (a) J. Wang, F. Wang, Z. Xu, Y. Wang and S. Dong, *Talanta* 2007, **74**, 104–109; (b) K. Kobayashi, N. Tonegawa, S. Fujii, J. Hikida, H. Nozoye, K. Tsutsui, Y. Wada, M. Chikira and M.-A. Haga, *Langmuir* 2008, **24**, 13203–13211; (c) M.-L. Ainalem, R. A. Campbell and T. Nylander, *Langmuir* 2010, **26**, 8625–8635; (d) J. Garcia–Castello, V. Toccafonde, J. Escorihuela, M. J. Bañuls, A. Maquieira and J. Garcia-Ruperez, *Opt. Lett*. 2012, **37**, 3684–3686.

7   (a) N. Gajovic-Eichelmann, E. Ehrentreich-Forster and F. F. Bier, *Biosens. Bioelect*ron. 2003, **19**, 417–422; (b) S. Pan and L. Rothberg, *Langmuir* 2005, **21**, 1022–1027 ; (c) A. Bonanni, M. I. Pividori and M. Valle, *Anal. Bioanal. Chem*. 2007, **389**, 851–861; (d) T. Arnandis-Chover, S. Morais, L. A. Tortajada-Genaro, R. Puchades, A. Maquieira, J. Berganza and G. Olabarria, *Talanta* 2012, **101**, 405–412.

8   (a) B. Bujoli, S. M. Lane, G. Nonglaton, M. Pipelier, J. Leger, D. R. Talham and C. Tellier, *Chem.-Eur. J*. 2005, **11**, 1980–1988; (b) C.-Y. Lee, P.-C. T. Nguyen, D. W. Grainger, L. J. Gamble and D. G. Castner, *Anal. Chem*. 2007, **79**, 4390–4400; (c) M. R. Lockett, M. F. Phillips, J. L. Jarecki, D. Peelen and L. M. Smith, *Langmuir* 2008, **24**, 69–75; (d) J. Timper, K. Gutsmiedl, C. Wirges, J. Broda, M. Noyong, J. Mayer, T. Carell and U. Simon, *Angew. Chem. Int. Ed*. 2012, **51**, 7586–7588.

9   E. S. Place, N. D. Evans and M. M. Stevens, *Nat. Mater*. 2009, **8**, 457–470.

10 A. Dondoni, *Angew. Chem. Int. Ed*. 2008, **47**, 8995–8997.

11 (a) H. C. Kolb, M. G. Finn and K. B. Sharpless, *Angew. Chem. Int. Ed*. 2001, **40**, 2004–2021; (b) C. E. Hoyle and C. N. Bowman, *Angew. Chem. Int. Ed*. 2010, **49**, 1540–1573.

12 (a) P.-C. Lin, D. Weinruch and H. Waldmann, Macromol. *Chem. Phys*. 2010, **211**, 136–144; (b) A. Bertin and H. Schlaad, *Chem. Mater*. 2009, **21**, 5698–5700; (c) D. Weinrich, P. C. Lin, P. Jonkheijm, U. T. T. Nuguyen, H. Schroder, C. M. Niemeyer, K. Alexandrov, R. Goody and H. Waldmann, *Angew. Chem. Int. Ed*. 2010, **49**, 1252–1257; (d) P. Jonkheijm, D. Weinrich, M. Kohn, H.

Engelkamp, P. C. M. Christianen, J. Kuhlmann, J. C. Maan, D. Nusse, H. Schroeder, R. Wacker, R. Breinbauer, C. M. Niemeyer and H. Waldmann, *Angew. Chem. Int. Ed*. 2008, **47**, 4421–4424; (e) M. A. Caipa Campos, J. M. J. Paulusse and H. Zuilhof, *Chem. Commun*. 2010, **46**, 5512–5514; (f) J. Escorihuela, M. J. Bañuls, R. Puchades and A. Maquieira, *Chem. Commun*. 2012, **48**, 2116–2118; (g) C. Wendeln, S. Rinnen, C. Schulz, T. Kaufmann, H. F. Arlinghaus and B. J. Ravoo, *Chem. Eur. J*. 2012, **18**, 5880–5888; (h) J. Escorihuela, M. J. Bañuls, S. Grijalvo, R. Eritja, R. Puchades and A. Maquieira, *Bioconjugate Chem*. 2014, **25**, 618–627.

13 (a) B. D. Fairbanks, E. A. Sims, K. S. Anseth and C. N. Bowman, *Macromolecules* 2010, **43**, 4113−4119; (b) N. S. Bhairamadgi, S. Gangarapu, M. A. Caipa Campos, J. M. J. Paulusse, C. J. M. van Rijn and Han Zuilhof, *Langmuir* 2013, **29**, 4535–4542.

14 (a) R. Hoogenboom, *Angew. Chem. Int. Ed*. 2010, **49**, 3415–3417; (b) A. Massi, D. Nanni, *Org. Biomol. Chem*. 2012, **10**, 3791–3807; (c) A. B. Lowe, C. E. Hoyle and C. N. Bowman, *J. Mat. Chem*. 2010, **20**, 4745–4750.

15 D. Mira, R. Llorente, S. Morais, R. Puchades, A. Maquieira and J. Marti, *Proc. SPIE*, 2004, **5617**, 364–373.

16 P. Xu, F. Huang and H. Liang, *Biosens. Bioelectron*. 2013, **41**, 505–510.

17 (a) S. J. Oh, S. J. Cho, C. O. Kim, and J. W. Park, *Langmuir* 2002, **18**, 1764–1769; (b) P. T. Charles, G. J. Vora, J. D. Andreadis, A. J. Fortney, C. E. Meador, C. S. Dulcey and D. A. Stenger, *Langmuir* 2003, **19**, 1586–1591; (c) A. Karsy, P. Borri, P. R. Davies, A. Harwood, N. Thomas, S. Lofas and T. Dale, *ACS Appl. Mater. Interfaces* 2009, **1**, 1793–1798; (d) R. A. Shircliff, P. Stradins, H. Moutinho, J. Fennell, M. L. Ghirardi, S. W. Cowley, H. M. Branz and I. T. Martin, *Langmuir* 2013, **29**, 4057–4067.

18 J. Escorihuela, M. J. Bañuls, R. Puchades and A. Maquieira, *Bioconjugate Chem*. 2012, **23**, 2121–2128.

19 (a) A. J. Haes and R. P. Van Duyne, *J. Am. Chem. Soc*. 2002, **124**, 10596–10604. (b) H. D. Inerowicz, S. Howell, F. E. Regnier, R. Reifenberger, *Langmuir* 2002, **18**, 5263–5268.

20 (a) S. Sun, D. Thompson, U. Schmidt, D. Graham and G. J. Leggett, *Chem. Commun*. 2010, **46**, 5292–5294; (b) A. Malainou, P. S. Petrou, S. E. Kakabakos, E. Gogolides and A. Tserepi, *Biosens. Bioelectron*. 2012, **34**, 273–281; (c) L. Feng, J. Romulus, M. Li, R. Sha, J. Royer, K.-T. Wu, Q. Xu. N. C. Seeman, M. Weck and P. Chaikin, *Nature Mater*. 2013, **12**, 747–454.

21 H. O. Ham, Z. Liu, K. H. A. Lau, and P. B. Messersmith, *Angew. Chem. Int. Ed*. 2011, **50**, 732–736.

22 M. Giesbers, A. T. M. Marcelis and H. Zuilhof, *Langmuir* 2013, **29**, 4782–4788.

23 (a) N. Graf, T. Gross, T. Wirth, W. Weigel and W. Unger, *Anal. Bioanal. Chem*. 2009, **393**, 1907–1912; (b) C.-Y. Lee, P. Gong, G. M. Harbers, D. W. Grainger, D. G. Castner and L. J. Gamble, *Anal. Chem*. 2006, **78**, 3316–3325.

24 J.-J. Chen, K. N. Struk and A. B. Brennan, *Langmuir* 2011, **27**, 13754–13761.

25 M. C. Pirrung, *Angew. Chem. Int. Ed*. 2002, **41**, 1276–1289.

26 (a) W. C. E. Schofield, J. McGettrick, T. J. Bradley, J. P. S. Badyal and S. Przyborski, *J. Am. Chem. Soc*. 2006, **128**, 2280–2285; (b) L.

G. Harris, W. C. E. Schofield, K. J. Doores, B. G. Davis and J. P. S. Badyal, *J. Am. Chem. Soc*. 2009, **131**, 7755–7761.

27 (a) G. H. Cross, N. J. Freeman and M. J. Swann, *in Handbook of Biosensors and Biochips*, ed. R. S. Marks, C. R. Lowe, D. C. Cullen, H. H. Weetall and I. Karube, John Wiley & Sons, New York, 2007, vol. 1, ch. 32, pp. 1–20; (b) G. H. Cross, Y. T. Ren and N. J. Freeman, *J. Appl. Phys.* 1999, **86**, 6483–6488.

28 (a) J. Escorihuela, M. J. Bañuls, J. García-Castelló, V. Toccafondo, J. García-Rupérez, R. Puchades and A. Maquieira, *Anal. Bioanal. Chem*. 2012, **404**, 2831–2840; (b) P. Xu, F. Huang and H. Liang, *Biosens. Bioelectron*. 2013, **41**, 505–510.

29 B. Rezek, D. Shin and C. E. Nebel, Langmuir 2007, 23, 7626–7633.

30 (a) J. H. Banoub, R. P. Newton, E. Esmans, D. F. Ewing and G. Mackenzie, *Chem. Rev*. 2005, **105**, 869–1915; (b) K. Wang, Z. Tang, C. J. Yang, Y. Kim, X. Fang, W. Li, Y. Wu, C. D. Medley, Z. Cao, J. Li, P. Colon, H. Lin and W. Tan, *Angew. Chem. Int. Ed*. 2009, **48**, 856–870.

31 H. I. Nakaya, E. M. Reis and S. Verjovski-Almeida *in Nucleic Acids Hybridization. Modern Applications*, A. Buzdin and S. Lukyanov, Springer, The Netherlands 2007, pp 265–307.

32 S. Morais, R. Marco-Molés, R. Puchades and A. Maquieira, *Chem. Commun*. 2006, 2368–2370.

33 S. C. Clarke, *Diagn. Microbiol. Infect. Dis*. 2001, **41**, 93–98.